


Cite this: *RSC Adv.*, 2020, 10, 26693

Received 4th March 2020

Accepted 28th June 2020

DOI: 10.1039/d0ra02051f

rsc.li/rsc-advances

# Oscillating syngas production on NiO/YSZ catalyst from methane oxidation†

Andrew C. Chien \*<sup>ab</sup> and Brian Y. Liao<sup>a</sup>

Synthesis gas was produced by methane oxidation on a NiO/YSZ cermet by interrupting the oxygen flow. Stopping the oxygen flow provoked the diffusion of lattice oxygen in the cermet, which in turn replenished the Ni–O bond that was consumed by methane. Resuming the oxygen flow brought about the activation of oxygen on the extrinsic vacancy site of YSZ. The activation, followed by the diffusion of oxygen and a Ni/NiO redox cycle, led to oscillatory syngas production. The infrared and mass spectroscopy results provide the reaction mechanism that governs the oxidation of methane on the NiO/YSZ cermet. This study presents a technique that can be applied to the catalysis of other metal/anion or cation conductor systems.

## Introduction

Nickel oxide/yttrium-stabilized zirconia (NiO/YSZ) is a state-of-the-art anode used in solid oxide fuel cells (SOFCs). Despite its excellent electrochemical activity in hydrogen fuel cells, there are barriers to the storage of hydrogen, which have stimulated interest in the investigation of chemical reactions on NiO/YSZ involving methane, a major component of natural gas. Many studies have shown that irreversible deactivation of the Ni/YSZ anode (after the reduction of NiO/YSZ) occurs due to the rapid pyrolysis of methane with carbon deposition.<sup>1,2</sup> The deposited carbon either encapsulates the active site of nickel or removes the nickel metal, thus leading to the destruction of the electrode microstructure and loss of conductivity. Moreover, the formation of carbon is very sensitive to temperature, the concentration of methane, the presence of steam, and the number of oxygen anions present. Consequently, the operation of the Ni/YSZ cermet as a component in an electrochemical cell is demanding. The search for alternative anode materials is widely recognized as an important technical objective in this field.<sup>3</sup>

On the other hand, the NiO/YSZ cermet is a potential metal supported catalyst for syngas production from methane oxidation.<sup>4,5</sup> Nickel is an active metal and can dissociate methane, and YSZ is an oxygen anion conductor, which can conduct oxygen through oxygen vacancies in the lattice. The oxidation of methane over a combination of Ni and YSZ can result in either the partial oxidation to synthesis gas or the full oxidation to carbon dioxide and water. Complete oxidation is expected to be

the main reaction occurring over oxide surfaces whereas the production of synthesis gas is more likely to occur over the metal surface. Two mechanisms for the partial oxidation of methane are proposed, namely direct and indirect synthesis.<sup>6,7</sup> In the indirect mechanism, the full oxidation products (CO<sub>2</sub> and H<sub>2</sub>O) react with unconverted methane to produce CO and H<sub>2</sub> *via* steam formation or dry reformation. However, this indirect mechanism can cause large temperature gradients and hotspots in the reactor because the exothermic deep oxidation and endothermic reforming reactions proceed in different zones of the reactor. In the direct mechanism, the synthesis gas is produced on a noble metal catalyst at a high temperature without the deep oxidation of methane. Nevertheless, the noble metal catalyst usually suffers from sintering and metal loss due to evaporation at high temperatures.<sup>8,9</sup>

Recently, we have shown that rhodium black partially covered with hexagonal boron nitride produces syngas by methane oxidation at 650 °C, following the interruption of the oxygen flow.<sup>10</sup> The absence of oxygen flow causes the surface oxides of the metal to reduce, thus allowing methane dissociation and the formation of a graphitic layer for syngas production. In this study, we adopted the same strategy by disturbing the oxygen flow to investigate methane oxidation on the NiO/YSZ cermet. By combining *in situ* infrared and mass spectroscopy, we showed that syngas is produced on the NiO/YSZ cermet in an oscillating mode and oxygen in nickel oxide is responsible for the oxidation of methane and the adsorption of the carbon species.

## Experimental

### Material synthesis

The nickel oxide/yttrium stabilized zirconia (NiO/YSZ) was prepared by the typical ceramic method as described in detail previously.<sup>11</sup> Nickel oxide (NiO; Novamet) and yttrium stabilized

<sup>a</sup>Department of Chemical Engineering, Feng Chia University, Taichung 40724, Taiwan. E-mail: cyinchien@fcu.edu.tw; Fax: +886 424510890; Tel: +886 424517250 ext 3691

<sup>b</sup>Green Energy Development Center, Feng Chia University, Taichung 40724, Taiwan

† Electronic supplementary information (ESI) available. See DOI: 10.1039/d0ra02051f



zirconia (13YSZ, Unitec Ceramics) were mixed (weight percent 50/50) in an organic solvent with an adequate amount of binder, dispersant (polyvinyl butyrate, Butvar B-98), plasticizer (dibutyl phthalate, DBP), and graphite as a pore former. The slurry mixture was ball-milled overnight, cast onto a tape using a doctor blade on a Mylar film, and then left to dry. The NiO/YSZ composite formed after the tape was removed from the Mylar film and calcined in air at 1400 °C for 4 h. The NiO/YSZ catalyst powder was obtained prior to the reaction studies by manually grinding the composite in an agate mortar.

### Partial methane oxidation

The oxidation of methane was conducted in a CATLAB system (Hidden Analytical) equipped with a plug-flow reactor and an integrated mass spectrometer. About 50 mg of the NiO/YSZ catalyst powder was loaded in a quartz reactor, which corresponded to a fixed GHSV of  $\sim 40\,000\text{ h}^{-1}$  and was heated with the reactant gas to the desired reaction temperature, *i.e.*, 650 °C. The reactant gases, CH<sub>4</sub> (4 sccm) and O<sub>2</sub> (2 sccm), diluted in helium (80 sccm) with a composition of  $\sim 5\text{ vol}\% \text{ CH}_4/2.5\text{ vol}\% \text{ O}_2/92.5\text{ vol}\% \text{ He}$ , were used without further purification. The composition of the reaction effluent was continuously monitored by mass spectrometry. The mass/electron ratios ( $m/z$ ) in MS were selected for H<sub>2</sub> (2), He (4), CH<sub>4</sub> (15), H<sub>2</sub>O (18), CO (28), O<sub>2</sub> (32), and CO<sub>2</sub> (44). The MS response for H<sub>2</sub> and CO was obtained by subtracting the CH<sub>4</sub> fragment intensity from the total MS response at  $m/z = 2$  and by subtracting the CO<sub>2</sub> fragment intensity from the total MS response at  $m/z = 28$ .

### In situ infrared spectroscopy studies

Diffuse Reflectance Infrared Fourier Transform Spectroscopy (DRIFTS) was used to investigate the reaction mechanism and intermediates of the oxidation of methane on NiO/YSZ catalysts. The infrared spectra were collected on a Thermo Nicolet iS10 infrared spectrometer attached to a diffuse reflection accessory (The Praying Mantis™, Harrick). An adequate amount of the catalyst powder was placed uniformly on a stainless steel high-temperature reaction chamber covered with a high-pressure dome. The chamber was purged with helium and then heated to 700 °C in the mixture of reactant gas. As the reaction reaches the steady state, the oxygen gas flow was interrupted for a period of  $\sim 30\text{--}60\text{ min}$ . *In situ* IR spectra were continuously recorded and monitored for changes in the adsorbed species on the catalyst and gas phase during the heating period and gas switching. In another study, a step reaction (methane–oxygen) was conducted to confirm the formation of a nickel–oxygen band *via* a redox reaction. The composition of the gas species eluting from the DRIFTS reactor was monitored by mass spectrometry (Hidden Analytical, HPR 20). The selected mass/electron ( $m/z$ ) ratio was the same as that used during the reaction.

### Pulse injection of O<sub>2</sub> and electrochemical measurement

Pulse reaction experiments and electrochemical studies were conducted on a NiO/YSZ anode supported cell sealed in a testing chamber. The details of the cell structure and testing

setup are described in previous work.<sup>12</sup> Prior to the pulse injection, the anode was reduced in H<sub>2</sub> (99.9%) at 700 °C to achieve complete reduction and then exposed to CH<sub>4</sub> (99.9%) for a certain period of time. As the oxygen was pulse injected onto the anode, the electric performance and gaseous products were monitored by a potentiostat and a mass spectrometer, respectively.

## Results

Fig. 1 shows the MS profiles of the gaseous products of methane oxidation on the NiO/YSZ catalysts at 650 °C. The MS profiles show that carbon dioxide and water are major oxidation products. The cession of the oxygen flow induced the dramatic production of carbon monoxide, which trends downward over time. Nevertheless, a spike in carbon monoxide production was observed periodically as the MS intensity of CO (*i.e.*, concentration) continued to decrease (Fig. 1b). Resuming the oxygen flow gave rise to rapid CO production, the intensity of which reached a plateau and proceeded in an oscillating fashion. Syngas was produced on this methane-exposed NiO/YSZ catalyst. Thereafter, the production of syngas oscillated in different periods from slow (10 min) to fast (3 min), as shown in Fig. 2.

Fig. 3(a) presents the *in situ* infrared spectra of the surface of the NiO/YSZ catalysts during the oxidation of methane upon heating to 650 °C. The spectra show that the bands of C–H bending and C–H stretching appear at 1350 and 3020 (cm<sup>−1</sup>),

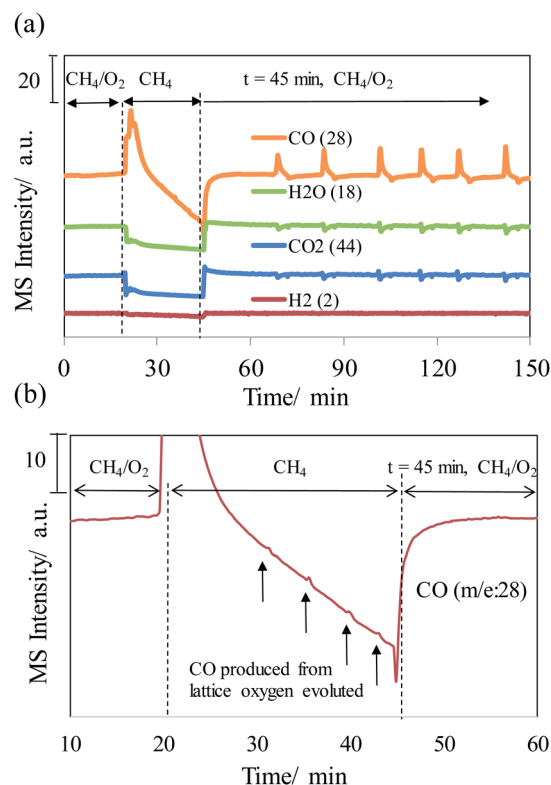


Fig. 1 (a) MS profiles of the gaseous products during the oxidation of methane on the NiO/YSZ catalysts at 650 °C, (b) MS profile of carbon monoxide, following the interruption of the oxygen stream.



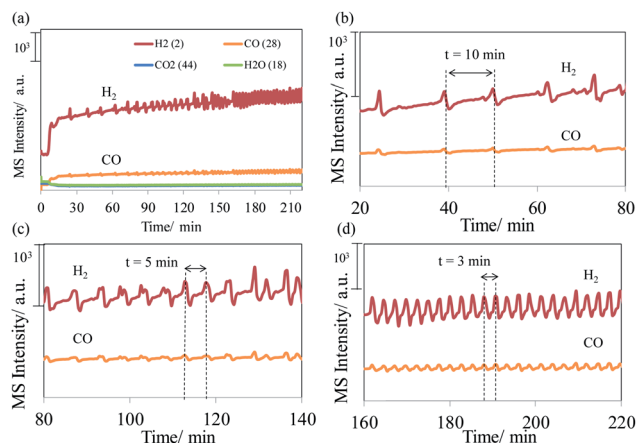


Fig. 2 MS profiles of the oscillating syngas production during the oxidation of methane on the NiO/YSZ catalysts at 650 °C.

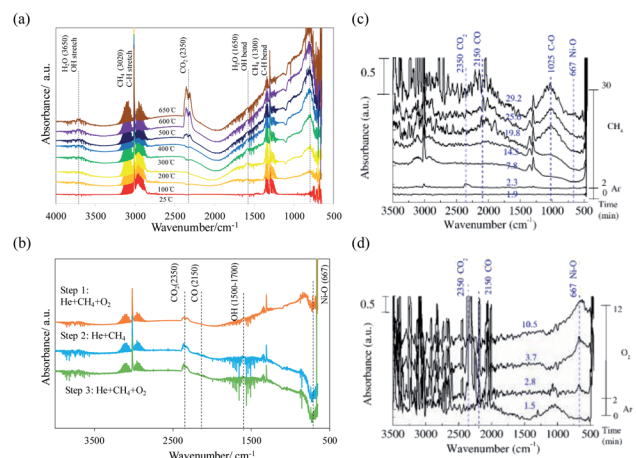


Fig. 3 *In situ* infrared spectra of the NiO/YSZ catalyst, (a) during the oxidation of methane upon heating, (b) after interrupting the oxygen flow, and IR spectra of the step reaction, (c) Ar-CH<sub>4</sub>, followed by (d) Ar-O<sub>2</sub> at 700 °C.

respectively, indicating the continuous introduction of methane. The major products of the oxidation of methane on the catalyst surface are carbon dioxide and dilute water. The peak intensity of both products increases as the temperature is elevated. When the oxygen flow is ceased, a band at 2150 cm<sup>-1</sup>, ascribed to gaseous carbon monoxide (CO), appeared, as shown in Fig. 3(b). In the absence of oxygen, the production of CO was accompanied by a decrease in the intensity of the nickel-oxygen band (Ni-O) at 667 cm<sup>-1</sup>.<sup>13,14</sup> The Ni-O band was not recovered during the oxidation of methane when the oxygen flow resumed. By contrast, the step reaction study on the NiO/YSZ catalyst showed that the decreased Ni-O band was regained in a pure oxygen atmosphere, as seen in Fig. 3(c) and (d). Nevertheless, the result verified the position of the Ni-O band since NiO is the only oxide that is reducible at the reaction temperature of the catalyst and no other metal-oxygen bonds are present due to the support metal oxide.

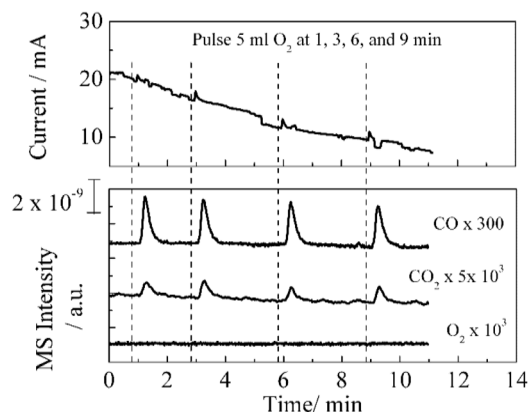


Fig. 4 CO production on the methane-exposed Ni/YSZ anode during O<sub>2</sub> pulses at 700 °C.

Fig. 4 shows the MS profiles and electric response during the pulse injection of O<sub>2</sub> onto a methane-exposed Ni/YSZ anode. A peak current together with the production of CO and CO<sub>2</sub> appeared after each pulse injection. Instead of CO<sub>2</sub>, CO was the major oxidation product of the pulse reaction. The production of the peak current implies that the injected oxygen was involved in electrochemical oxidation. The activation of gaseous oxygen on the electrode and subsequent diffusion through the lattice vacant sites probably occurred, thereby enhancing CO production.

## Discussion

The catalytic partial oxidation of methane is known to produce syngas and syngas-derived chemicals over transition metal catalysts. The literature presents theoretical and experimental evidence pointing to the inherent differences between the reaction mechanisms of different metal catalysts. These differences are related to the activation of the C-H bonds, *i.e.*, the dissociation of methane, stability of the surface species, residence time, and participation of lattice oxygen in the support oxides. CO<sub>2</sub> and H<sub>2</sub>O are the main reaction products at low temperatures or on an oxidized surface. Syngas (H<sub>2</sub> and CO) emanates from the dissociation of methane on a reduced metal surface and subsequent oxidative conversion of the active species. At elevated temperatures, oxides of the active species may be directly reduced by interaction with methane or through reaction with pyrolyzed products such as H<sub>2</sub> and C. Moreover, higher temperatures also shift the equilibrium of the reaction to produce CO rather than CO<sub>2</sub>. Since partial methane oxidation is an exothermic reaction, heat and mass transfer both play a role in the reaction mechanism and product distribution.

### Evolution of CO from lattice oxygen

Experimental results revealed that the oxidation of methane on the NiO/YSZ cermet produces syngas rather than carbon dioxide and water after interrupting the oxygen flow. The production of syngas inferred that methane underwent partial oxidation when the oxygen flow resumed. Notably, this is different from the reaction before the interruption. The change in the reaction products, as well as the mechanism, arose due to the absence of



oxygen and exposure of the NiO/YSZ cermet to a reducing atmosphere for a period of time. In the absence of oxygen, the NiO/YSZ cermet was reduced as oxygen was extracted by methane, thus giving a burst of carbon monoxide production (Fig. 1a). As the cermet became oxygen deficient on the surface, lattice oxygen in the yttrium stabilized zirconia diffused to replenish the supply. The lattice oxygen then reacted with methane, resulting in a spike in carbon monoxide production in a periodic manner (Fig. 1b). This suggested that the rate of CO production is limited either due to the sluggish oxidation reaction or oxygen supply. The rate-limiting mechanism was still maintained even though a sufficient amount of gaseous oxygen was available again. The MS result showed that resuming the oxygen flow caused a rapid increase in the carbon monoxide intensity, accompanied by a periodic pattern of spiked production, as before. Later, oscillating syngas production was observed. The oscillating production of syngas showed nonlinear dynamics far from equilibrium. The frequency of the oscillation increased as the time interval (peak to peak) shortened during the oxidation reaction (Fig. 2). The nonlinear dynamics of heterogeneous catalysis is known to exhibit complex temporal and spatiotemporal behaviour.<sup>15</sup> One example of this is surface restructuring on metal catalysts, *e.g.* platinum and palladium, induced by CO oxidation.<sup>16</sup> Nevertheless, the oscillatory behavior observed in the current system is more likely related to the transport of lattice oxygen and the resulting surface reaction on the nickel metal. Studies on isotopic exchange reactions demonstrated that methane is selectively oxidized by lattice oxygen on the surface of zirconia and yttrium-stabilized zirconia.<sup>17,18</sup> The partial oxidation of methane on YSZ proceeds *via* the Mars–van Krevelen mechanism.<sup>6,19</sup> Therefore, a similar mechanism is expected to occur on the methane-exposed NiO/YSZ cermet in this study.

### Mechanism of oscillating syngas production

A reaction mechanism is speculated to explain the production of the syngas and its oscillatory behavior, as shown in Fig. 5.

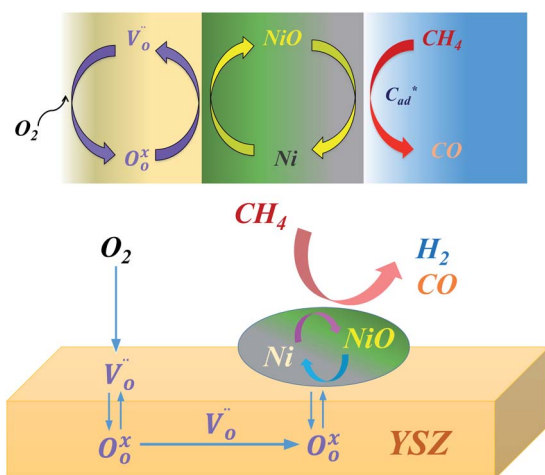


Fig. 5 Proposed reaction mechanism for the oxidation of methane for oscillating syngas production on the NiO/YSZ catalyst.

The mechanism consists of several steps, including the (i) activation of oxygen, (ii) diffusion of lattice oxygen, (iii) oxidation of the nickel metal site, and (iii) extraction of oxygen from the Ni–O bond by methane. The interruption of the oxygen flow caused the extraction of oxygen on the metal site of Ni/YSZ by CH<sub>4</sub>, thus provoking the diffusion of oxygen ions in the lattice. The diffusion process did not occur when the cermet was in the presence of CH<sub>4</sub> and O<sub>2</sub>. Restoring the oxygen initiated the activation of oxygen at extrinsic oxygen vacancies on the surface of YSZ. The activation of oxygen, in conjunction with the diffusion, led to the replenishment of oxygen for the nickel–oxygen bond consumed by methane. The deprivation of oxygen in NiO/YSZ is evident as extensive exposure to CH<sub>4</sub> continued to decrease the Ni–O band in the DRIFTS spectra (Fig. 3). However, the decreased Ni–O band was not recovered after the restoration of the O<sub>2</sub> gas flow. This infers that the gaseous oxygen is probably engaged in vacancy activation instead of the oxidation of the metal, thus the formation of Ni–O bonds was not observed. On the other hand, the extraction of oxygen may be faster than the diffusion of oxygen in the lattice. Thus, the changes in the Ni–O band could not be detected. In another study, Jin *et al.*<sup>20</sup> used a pulse reactor to study the mechanism of the oxidation of methane on Ni/Al<sub>2</sub>O<sub>3</sub> and reported that, over reduced nickel, the dissociation of gaseous oxygen did not result in NiO but rather Ni<sup>δ+</sup>–O<sup>δ–</sup> species were produced. The reaction between Ni<sup>δ+</sup>–O<sup>δ–</sup> and Ni–carbon intermediates claimed to yield CO as the primary product. As a result, the oscillatory behavior of syngas production resulted from the redox cycle of Ni and NiO, which is affected by the kinetics of oxygen extraction, oxygen supply, vacancy activation, and the mass transfer of the lattice oxygen anion.<sup>21,22</sup>

Moreover, the involvement of lattice oxygen in the reaction was evidenced by enhanced CO production during the pulse injection of O<sub>2</sub> on methane-exposed Ni/YSZ (Fig. 4), which is attributed to the effects of electrochemical promotion.<sup>23,24</sup> The involvement of lattice oxygen in heterogeneous catalysis (carbon pathways of methane dry reforming) was recently reported, where the removal of carbon species and production of CO was monitored using transient techniques on titanium doped ceria.<sup>25,26</sup> The oscillatory behavior of the Ni–YSZ anode during the oxidation of methane was also reported in an electrochemical cell using *in situ* electrochemical methods.<sup>27,28</sup> These phenomena are regarded as repetitive cycles of oxidation and reduction on the metal surface. Moreover, during the production of the gaseous products of methane oxidation, oscillations also occur on nickel foil and powdered catalysts.<sup>29,30</sup> The cause of these oscillations depends on the activities of the metal/metal oxide, temperature, and the concentration of oxygen, which in turn affects the frequency and amplitude of an oscillating wave.<sup>31</sup>

## Conclusions

In conclusion, we showed that syngas can be produced on a NiO/YSZ cermet *via* the Mars–van Krevelen mechanism. On the NiO/YSZ cermet, CO<sub>2</sub> and H<sub>2</sub>O were the major products in methane oxidation. In contrast, CO and H<sub>2</sub> were produced after





the oxygen gas flow was interrupted. The production of syngas proceeded in an oscillating mode, which was attributed to oxygen diffusion in the lattice and the redox cycle of Ni and NiO. *In situ* DRIFTS results determined that the Ni–O bonds on the cermet are deprived of oxygen during the oxidation of methane on the surface. The MS and electrochemical tests revealed that lattice oxygen also plays a role in the reaction. The results reported herein are applicable to oxidation reactions of other combinations of metals and oxygen anion conductors. Furthermore, this combination concept can be expanded to catalysis with cation conductors, such as proton conductors for hydrogenation reactions.

## Conflicts of interest

There are no conflicts to declare.

## Acknowledgements

The authors would like to acknowledge the financial support from Feng Chia University and from Taiwan Ministry of Science and Technology under contract MOST 106-2218-E-035-009-MY2.

## References

- 1 S. Somacescu, N. Cioatera, P. Osiceanu, J. M. Calderon-Moreno, C. Ghica, F. Neațu and M. Florea, Bimodal mesoporous NiO/CeO<sub>2-δ</sub>-YSZ with enhanced carbon tolerance in catalytic partial oxidation of methane-Potential IT-SOFCs anode, *Appl. Catal., B*, 2019, **241**, 393–406.
- 2 N. C. Triantafyllopoulos and S. G. Neophytides, The nature and binding strength of carbon ad species formed during the equilibrium dissociative adsorption of CH<sub>4</sub> on Ni-YSZ cermet catalysts, *J. Catal.*, 2003, **217**, 324–333.
- 3 W. Wang, C. Su, Y. Wu, R. Ran and Z. Shao, Progress in solid oxide fuel cells with nickel-based anodes operating on methane and related fuels, *Chem. Rev.*, 2013, **113**, 8104–8151.
- 4 Y. Wang, W. Wang, X. Hong, Y. Li and Z. Zhang, Yttrium-stabilized zirconia-promoted metallic nickel catalysts for the partial oxidation of methane to hydrogen, *Int. J. Hydrogen Energy*, 2009, **34**, 2252–2259.
- 5 Y. Lin, Z. Zhan, J. Liu and S. A. Barnett, Direct operation of solid oxide fuel cells with methane fuel, *Solid State Ionics*, 2005, **176**, 1827–1835.
- 6 E. I. Kauppi, K. Honkala, A. O. I. Krause, J. M. Kanervo and L. Lefferts, ZrO<sub>2</sub> Acting as a Redox Catalyst, *Top. Catal.*, 2016, **59**, 823–832.
- 7 B. Christian Enger, R. Lødeng and A. Holmen, A review of catalytic partial oxidation of methane to synthesis gas with emphasis on reaction mechanisms over transition metal catalysts, *Appl. Catal., A*, 2008, **346**, 1–27.
- 8 E. D. Goodman, A. A. Latimer, A.-C. Yang, L. Wu, N. Tahsini, F. Abild-Pedersen and M. Cargnello, Low-Temperature Methane Partial Oxidation to Syngas with Modular Nanocrystal Catalysts, *ACS Appl. Nano Mater.*, 2018, **1**, 5258–5267.
- 9 V. A. Kondratenko, C. Berger-Karin and E. V. Kondratenko, Partial oxidation of methane to syngas over  $\gamma$ -Al<sub>2</sub>O<sub>3</sub>-supported Rh nanoparticles: Kinetic and mechanistic origins of size effect on selectivity and activity, *ACS Catal.*, 2014, **4**, 3136–3144.
- 10 A. C. Chien and J. A. Van Bokhoven, Boron nitride coated rhodium black for stable production of syngas, *Catal. Sci. Technol.*, 2015, **5**, 3518–3524.
- 11 A. C. Chien, A. Arenillas, C. Jiang and J. T. S. Irvine, Performance of direct carbon fuel cells operated on coal and effect of operation mode, *J. Electrochem. Soc.*, 2014, **161**, F588–F593.
- 12 A. C. Chien and S. S. C. Chuang, Effect of gas flow rates and Boudouard reactions on the performance of Ni/YSZ anode supported solid oxide fuel cells with solid carbon fuels, *J. Power Sources*, 2011, **196**, 4719–4723.
- 13 A. Citra, G. V. Chertihin, L. Andrews and M. Neurock, Reactions of laser-ablated nickel atoms with dioxygen. Infrared spectra and density functional calculations of nickel oxides NiO, ONiO, Ni<sub>2</sub>O<sub>2</sub>, and Ni<sub>2</sub>O<sub>3</sub>, superoxide NiOO, peroxide Ni(O<sub>2</sub>), and higher complexes in solid argon, *J. Phys. Chem. A*, 1997, **101**, 3109–3118.
- 14 V. Biju and M. Abdul Khadar, Fourier transform infrared spectroscopy study of nanostructured nickel oxide, *Spectrochim. Acta, Part A*, 2003, **59**, 121–134.
- 15 R. Imbihl, Nonlinear dynamics on catalytic surfaces: The contribution of surface science, *Surf. Sci.*, 2009, **603**, 1671–1679.
- 16 M. A. Van Spronsen, J. W. M. Frenken and I. M. N. Groot, Surface science under reaction conditions: CO oxidation on Pt and Pd model catalysts, *Chem. Soc. Rev.*, 2017, **46**, 4347–4374.
- 17 J. Zhu, J. G. Van Ommen, H. J. M. Bouwmeester and L. Lefferts, Activation of O<sub>2</sub> and CH<sub>4</sub> on yttrium-stabilized zirconia for the partial oxidation of methane to synthesis gas, *J. Catal.*, 2005, **233**, 434–441.
- 18 C. Kokkoffitis and M. Stoukides, Rate and oxygen activity oscillations during propane oxidation on Pt/YSZ, *J. Catal.*, 2006, **243**, 428–437.
- 19 C. Doornkamp and V. Ponec, The universal character of the Mars and Van Krevelen mechanism, *J. Mol. Catal. A: Chem.*, 2000, **162**, 19–32.
- 20 R. Jin, Y. Chen, W. Li, W. Cui, Y. Ji, C. Yu and Y. Jiang, Mechanism for catalytic partial oxidation of methane to syngas over a Ni/Al<sub>2</sub>O<sub>3</sub> catalyst, *Appl. Catal., A*, 2000, **201**, 71–80.
- 21 A. R. Puigdollers, P. Schlexer, S. Tosoni and G. Pacchioni, Increasing oxide reducibility: The role of metal/oxide interfaces in the formation of oxygen vacancies, *ACS Catal.*, 2017, **7**, 6493–6513.
- 22 S. Kwon, P. Deshlahra and E. Iglesia, Dioxygen activation routes in Mars-van Krevelen redox cycles catalyzed by metal oxides, *J. Catal.*, 2018, **364**, 228–247.
- 23 T. J. Huang and M. C. Huang, Electrochemical promotion of bulk lattice-oxygen extraction for direct methane conversion to syngas in SOFCs with Ni-YSZ anodes, *Chem. Eng. J.*, 2008, **138**, 538–547.



- 24 J. Nicole, C. Comninellis, D. Tsiptrakides, C. Pliangos, X. E. Verykios and C. G. Vayenas, Electrochemical promotion and metal-support interactions, *J. Catal.*, 2001, **204**, 23–34.
- 25 M. A. Vasiliades, C. M. Damaskinos, K. K. Kyprianou, M. Kollia and A. M. Efstathiou, The effect of Pt on the carbon pathways in the dry reforming of methane over Ni-Pt/Ce<sub>0.8</sub>Pr<sub>0.2</sub>O<sub>2-δ</sub> catalyst, *Catal. Today*, 2019, DOI: 10.1016/j.cattod.2019.04.022.
- 26 C. M. Damaskinos, M. A. Vasiliades and A. M. Efstathiou, The effect of Ti<sup>4+</sup> dopant in the 5 wt% Ni/Ce<sub>1-x</sub>Ti<sub>x</sub>O<sub>2-δ</sub> catalyst on the carbon pathways of dry reforming of methane studied by various transient and isotopic techniques, *Appl. Catal., A*, 2019, **579**, 116–129.
- 27 D. Lee, D. Kim, J. Kim and J. Moon, Characterizing nano-scale electrocatalysis during partial oxidation of methane, *Sci. Rep.*, 2014, **4**, 3937.
- 28 Z. H. Wang, Z. Lu, K. F. Chen, B. Wei, X. B. Zhu, X. Q. Huang and W. H. Su, Redox tolerance of thin and thick Ni/YSZ anodes of electrolyte-supported single-chamber solid oxide fuel cells under methane oxidation conditions, *Fuel Cells*, 2013, **13**, 1109–1115.
- 29 X. Zhang, C. S. M. Lee, D. O. Hayward and D. M. P. Mingos, Oscillatory behaviour observed in the rate of oxidation of methane over metal catalysts, *Catal. Today*, 2005, **105**, 283–294.
- 30 M. M. Slinko, V. N. Korchak and N. V. Peskov, Mathematical modelling of oscillatory behaviour during methane oxidation over Ni catalysts, *Appl. Catal., A*, 2006, **303**, 258–267.
- 31 X. Ren and X. Guo, Effect of heat transfer on the oscillatory behavior in partial oxidation of methane over nickel catalyst, *J. Nat. Gas Chem.*, 2011, **20**, 503–506.

